Density distribution of ^{17}B from a reaction cross-section measurement

Y. Yamaguchi,[1,2,*] C. Wu,[1,3] T. Suzuki,[2,†] A. Ozawa,[1,‡] D. Q. Fang,[1,4] M. Fukuda,[5] N. Iwasa,[6] T. Izumikawa,[2] H. Jeppesen,[1,7] R. Kanungo,[1] R. Koyama,[2] T. Ohnishi,[1] T. Ohtsubo,[2] W. Shinozaki,[2] T. Suda,[1] M. Takahashi,[2] and I. Tanihata[1,§]

[1]*The Institute for Physical and Chemical Research (RIKEN), Saitama 351-0198, Japan*
[2]*Department of Physics, Niigata University, Niigata 950-2181, Japan*
[3]*School of Physics, Peking University, Beijing 100871, China*
[4]*Shanghai Institute of Nuclear Research, Chinese Academy of Sciences, Shanghai 201800, China*
[5]*Department of Physics, Osaka University, Osaka 560-0043, Japan*
[6]*Department of Physics, Tohoku University, Miyagi 980-8578, Japan*
[7]*Department of Physics and Astronomy, University of Aarhus, DK-8000 Aarhus C, Denmark*

(Received 22 July 2004; published 24 November 2004)

The reaction cross section (σ_R) for the neutron-rich nucleus ^{17}B on a carbon target has been measured at an energy of 77*A* MeV by the transmission method. An enhancement of σ_R at intermediate energy compared to that at high energy was observed. The density distribution of ^{17}B was deduced through the energy dependence of σ_R using a finite-range Glauber-type calculation under an optical-limit approximation as well as a few-body approach. The existence of a long neutron tail in ^{17}B was demonstrated. The fraction of the wave function with the valence two-neutron configuration of $(2s_{1/2})^2_{J=0}$ or $(1d_{5/2})^2_{J=0}$ was found to be $50\pm10\%$ based on a finite-range few-body Glauber-type calculation.

DOI: 10.1103/PhysRevC.70.054320 PACS number(s): 21.10.Gv, 25.60.Dz, 27.20.+n

I. INTRODUCTION

During the last few decades investigations of unstable nuclei have made rapid progress by means of a radioactive ion-beam technique. After the neutron halo in ^{11}Li was discovered [1,2], the existence of a neutron halo in some neutron-rich light nuclei was suggested. The neutron halo, established in ^{11}Li and in ^{11}Be [3–11], can be characterized by a weak binding energy of the valence neutron(s), a large matter radius, and a narrow momentum distribution following fragmentation. An *s*-wave dominance in valence neutron(s) plays an essential role in halo formation.

From a theoretical point of view, ^{17}B ($J^\pi=3/2^-$, $T_{1/2}=5.08$ ms [12]) is considered to be a three-body system composed of the $A=3Z$ core and two outside neutrons [13]. Riisager *et al.* have classified halo states by using a universal-scaling plot for three-body systems with hyperangular momentum (K) [14]. The quantum number K is 0, 1, and 2, depending on whether the two neutrons are in *s* waves, roughly half of the *s* wave plus half of the *pd* wave, and mainly *pd* waves, respectively, relative to the core. Thus, the states with $K=0$ and 1 can contribute to halo formation. According to their argument, ^{17}B can be classified into the category with the $K=1$ state. Therefore, it is expected to be a halo nucleus.

Experimentally, ^{17}B has been suggested to be a two-neutron halo nucleus due to its weak binding of the valence two-neutron ($S_{2n}=1.39\pm0.14$ MeV) [15], the large root-mean-square (rms) matter radius ($\tilde{r}=2.90\pm0.06$ fm) [16], and the narrow momentum distribution of ^{15}B fragments ($\Gamma=80\pm10$ MeV/c) [17] from the breakup of ^{17}B.

Motivated by the theoretical argument and the measurements mentioned above, we studied the density distribution of ^{17}B to understand the halo structure. The existence of a long neutron tail in ^{17}B as well as its amplitude and the fraction of the wave function with the valence two-neutron configuration are discussed in this report.

II. EXPERIMENT

The experiment was performed at the RIKEN projectile fragment separator (RIPS) [18]. The experimental setup is shown in Fig. 1.

A Be (739 mg/cm^2 thick) or Ta (1498 mg/cm^2 thick) target was installed in the F0 area as a production target. We installed an Al wedge degrader and a parallel-plate avalanche counter (PPAC) [19] at the F1 dispersive focus. A carbon (C) reaction target (377 mg/cm^2 thick) was placed at the F2 achromatic focus. Two PPACs, a silicon detector ($50\times50\times0.15$ mm^3), and a plastic scintillator (0.5 mm thick) were installed in the front of the reaction target. Two PPACs, a plastic scintillator (1.5 mm thick), and a tilted-electrode gas ionization chamber (TEG-IC) [20] were placed at the F3 focus (in order looking upstream). TEG-IC was filled with a counting gas [Ar-CH$_4$(90%,10%)] with effective length 650 mm (ϕ=90 mm). A $3''\phi\times6$ cm NaI(Tl) detector was placed at the end of the beam line surrounded by reaction suppressors. The reaction suppressors were plastic scintilla-

*Present address: Center for Nuclear Study (CNS), University of Tokyo RIKEN campus, Saitama 351-0198, Japan.

†Present address: Department of Physics, Saitama University, Saitama 338-8570, Japan.

‡Present address: Institute of Physics, University of Tsukuba, Ibaraki 305-8571, Japan.

§Present address: Physics Division, Argonne National Laboratory, Argonne, Illinois 60439, USA.

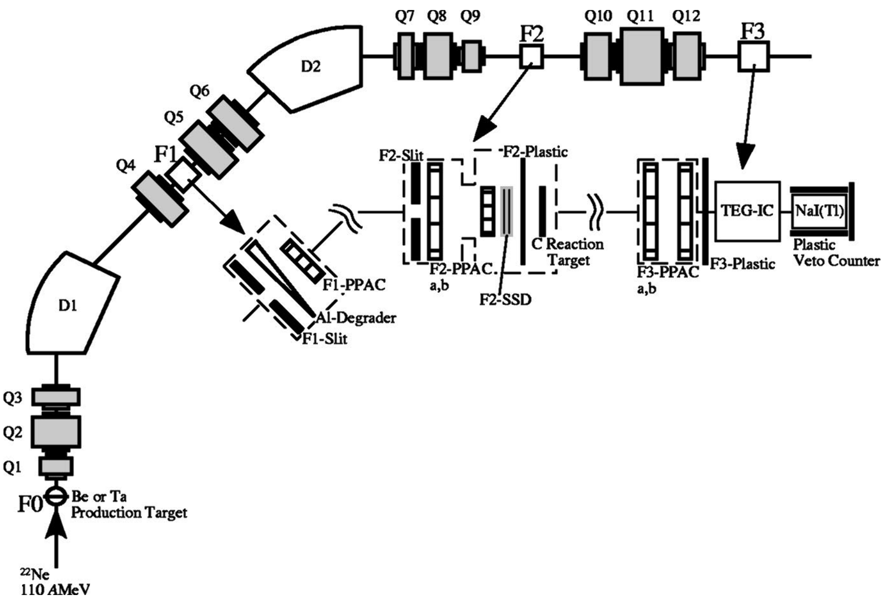

FIG. 1. Experimental setup at RIPS.

tion counters which detected the emitted charged particles or neutrons from reactions in the NaI(Tl).

Particles were identified event by event. A nucleus before the reaction target was identified by the magnetic rigidity ($B\rho$), energy loss (ΔE), and time of flight (TOF) measured for each fragment. The $B\rho$ was determined by position information from a PPAC. The magnetic fields at the two dipole magnets were monitored by NMR probes, and ΔE was measured using the silicon detector. TOF information before the reaction target was determined by using the rf signal and the timing signal from the plastic scintillator at F2.

A nucleus after the reaction target was identified by its TOF, ΔE, and total energy (E). The TOF information was obtained between two plastic scintillators, one at F2 and the other at F3. ΔE was measured by the TEG-IC, and E was measured by the NaI(Tl) detector.

After the selection of $Z=5$ particles using ΔE information from TEG-IC, particles were identified by using TOF-corrected E information from the NaI(Tl), as shown in Fig. 2. A long tail towards the low-energy side and a small tail on the high-energy side, as shown by the dotted line in Fig. 2, are due to products of the nuclear reaction inside NaI(Tl), and this is the main background for estimating the number of fragments. In order to reduce this background as much as possible, we used the reaction suppressors mentioned above. Events could be removed offline if a signal due to charged particles and/or neutrons produced inside the NaI(Tl) was recorded in the reaction suppressors. The fragments ^{13,14,15}B could be clearly separated from the ^{17}B, as shown by the solid line in Fig. 2.

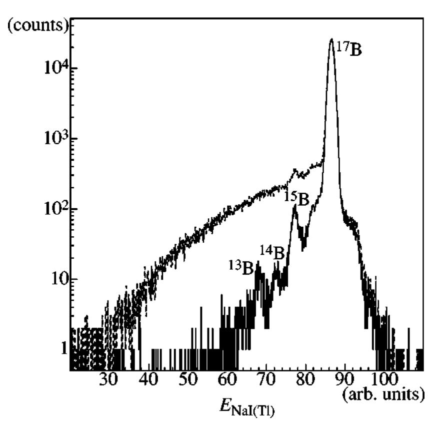

FIG. 2. Particle identification of unreacted ^{17}B and fragments from the breakup of ^{17}B. Fragments other than $Z=5$ are already subtracted. The dotted and solid lines show the energy spectrum without and with the reaction suppression, respectively.

III. RESULTS AND DISCUSSION

A. Reaction cross section

We measured the reaction cross section of ^{17}B on the C reaction target by the transmission method. An incident primary beam of ^{22}Ne with 110A MeV accelerated by the RIKEN ring cyclotron, was directed onto the Be or Ta production target to produce ^{17}B as a secondary beam. The ^{17}B secondary beam was transported from the F0 area to the F3 focus by using the achromatic operating mode of RIPS. Measurements with and without the reaction target were performed using the combinations of the Ta (Be) production target and Al wedge degrader with central thickness of 1244 mg/cm^2(2147 mg/cm^2), in order to correct for energy loss in the reaction target. The ^{17}B beam energy was 77A MeV in the middle of the reaction target. The ^{17}B beam intensity was around 200 counts/s and its purity was around 70% with a typical primary beam intensity of 300 pnA.

The reaction cross section (σ_R) of ^{17}B was determined by

$$\sigma_R = -\frac{1}{t}\ln\left(\frac{R_{in}}{R_{out}}\right), \qquad (1)$$

where t denotes the reaction target thickness in units of atom/cm^2; R_{in} and R_{out} are the ratios of the number of outgoing unreacted ^{17}B to that of an incident ^{17}B with and without the reaction target, respectively. It should be noted here that the outgoing particles include not only the unreacted ^{17}B

TABLE I. $\sigma_R(^{17}\mathrm{B})$ at intermediate energy and $\sigma_I(^{17}\mathrm{B})$ at high energy on a carbon target.

Energy (A MeV)	σ_R(mb)	σ_I(mb)
77	1400±29	
880		1118±22[a]

[a]Reference [16].

but also any inelastic events and other fragments. The number of outgoing unreacted ^{17}B was determined by subtracting the inelastic events and other fragments from $Z=5$ outgoing nuclei. Therefore, we carefully estimated the inelastic events and the number of other fragments by using TOF information (please refer to Ref. [21] for details).

The resultant σ_R at 77A MeV was determined to be 1400±29 mb and is shown in Table I along with the previous result of the interaction cross section (σ_I) at high energy (880A MeV), which was measured at GSI [16].

The statistical error of the present measurement, which depends on the uncertainty of $R_{in,out}$, was estimated to be ±19 mb in σ_R by using a binomial distribution for the outgoing particles. As for the other uncertainties, we considered the following: (1) Contamination of the incident particles, which stems from the reacted events in the silicon detector. The ratio of contaminants to the incident ^{17}B was estimated to be 1.69×10^{-4} in an offline analysis. The error due to this uncertainty was estimated to be ±9 mb in σ_R. (2) The error arising from the measurement of the reaction-target thickness was estimated to be ±1 mb in σ_R. (3) The error in the estimation of the number of fragments (^{13,14,15}B) and the ambiguity of its method was estimated to be ±7 mb in σ_R. (4) The error due to the uncertainty in the estimation of the inelastic events has a large influence on σ_R, like the statistical error mentioned above. We used the value of the half of the difference between the lower limit and upper limit of the estimation as the error, which was ±18 mb in σ_R.

We did find an enhancement of σ_R compared with that of the value predicted by a phenomenological formula, proposed by Kox *et al.* [22]. The phenomenological formula can well reproduce σ_R for stable nuclei. The measured σ_R and the expected values from the phenomenological formula are shown in Fig. 3.

As a derived from Ref. [23], σ_I can be treated as σ_R at relativistic energies (high energies). The enhancement of the measured σ_R at intermediate energy is much larger than that at high energy. This fact implies the existence of a long tail at a large distance from the center of the nucleus, since the σ_R at intermediate energies are expected to be more sensitive to the outer part of nucleus than those at high energies [5].

B. Glauber-model analysis

The Glauber-type calculation is a useful tool, which associates σ_R and a density distribution $[\rho(r)]$ in a high-energy region, and has been widely used so far. Under the optical-limit (OL) approximation, σ_R is calculated by

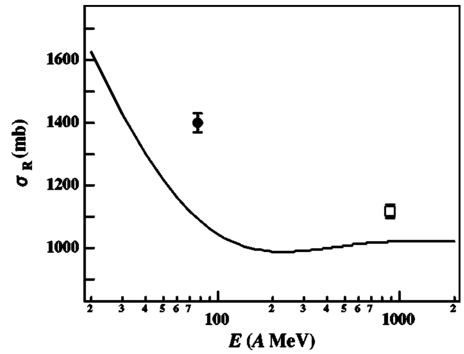

FIG. 3. Measured σ_R as a function of the incident beam energy. The closed circle shows the present measurement, and the open square shows the previous measurement [16]. The expected value from the phenomenological formula is shown by the solid line.

$$\sigma_R^{\mathrm{OL}} = 2\pi \int db\, b[1 - T(b)]C(E), \tag{2}$$

where $C(E)$ denotes the influence of the Coulomb force. Here, $T(b)$ is the transmission, which is given by

$$T(b) = \exp\left\{ - \int\int \sum_{ij} [\Gamma_{ij}(\boldsymbol{b}+\boldsymbol{s}-\boldsymbol{t})\rho_{Ti}^z(\boldsymbol{t})\rho_{Pj}^z(\boldsymbol{s})]d\boldsymbol{s}\, d\boldsymbol{t} \right\}, \tag{3}$$

where Γ_{ij} is the profile function and $\boldsymbol{b}$ is the impact parameter; $\boldsymbol{s}$ and $\boldsymbol{t}$ denote the two-dimensional nucleon vectors in the projectile and target nuclei, respectively, perpendicular to the beam axis. ρ_{Pj}^z and ρ_{Ti}^z are the z integrated density of the projectile and the target nuclei, respectively.

At an intermediate energy region, however, it is known that the calculated σ_R^{OL} underestimates the experimental σ_R, even for a stable ^{12}C+^{12}C system. Zheng *et al.* took a finite-range effect of nucleon-nucleon (NN) collisions into account using a profile function [24] to correct the underestimation. It is parameterized in the form of

$$\Gamma_{ij}(\boldsymbol{b}) = \frac{1 - i\alpha}{4\pi\beta_{ij}^2}\sigma_{ij}(E)\exp\left(-\frac{\boldsymbol{b}^2}{2\beta_{ij}^2}\right), \tag{4}$$

where $\sigma_{ij}(E)$ is the NN total cross section and β_{ij} is understood to be the range of interaction between NN [25], the so-called finite-range parameter; α is the ratio between the real and imaginary parts of the NN scattering amplitude at zero degrees. Since we calculated only σ_R, we did not need to take α into account. We parametrized a new finite-range parameter by fitting the energy dependence of σ_R for the ^{12}C+^{12}C system, including new data from Ref. [26]. It can be expressed as

$$\beta_{ij} = 0.56288 \exp\left[-\left(\frac{E - 36.932}{169.86}\right)^2\right] + 0.11743. \tag{5}$$

The calculated σ_R^{OL} for the ^{12}C+^{12}C system is shown in Fig. 4(b). The experimental σ_R of ^{12}C is well reproduced if a finite-range parameter is introduced.

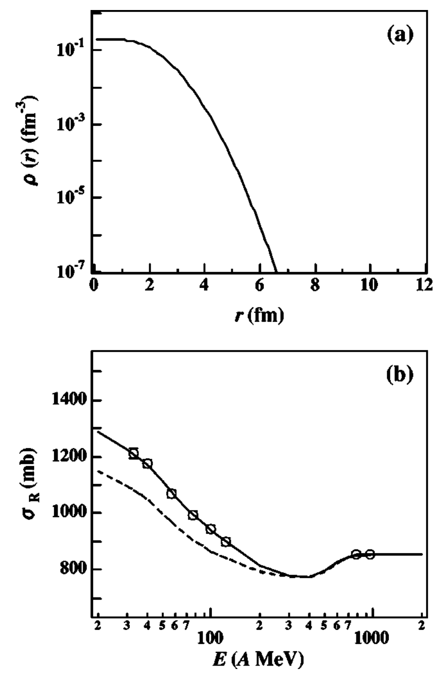

FIG. 4. (a) The assumed $\rho(r)$ of ^{12}C is a HO-type function. The width parameter (a_{HO}) of the HO-type $\rho(r)$ was chosen to be 1.571 fm to reproduce the rms radius determined by the electron scattering experiment. (b) Energy dependence of σ_R for the $^{12}\mathrm{C}+^{12}\mathrm{C}$ system. The open circles show the experimental data, where the data at intermediate energy are taken from Ref. [26] and those at high energy are taken from Ref. [27]. The dashed and solid lines stand for the calculation under the OL approach with zero-range ($\beta_{ij}=0$) and finite-range treatment, respectively.

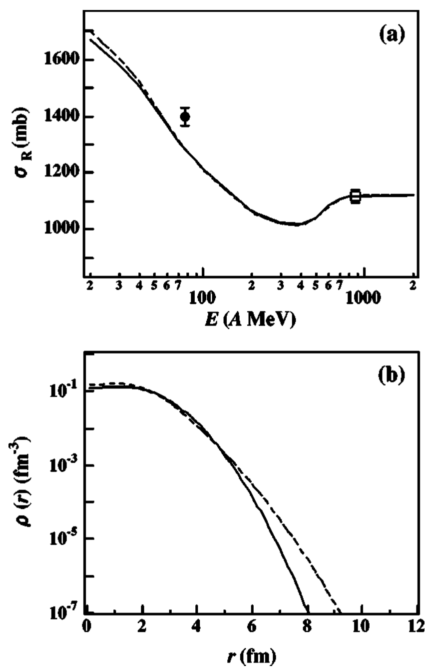

FIG. 5. (a) Energy dependence of σ_R for ^{17}B. The points are measured values and the symbols are the same as those in Fig. 3. The dashed and solid lines are the result of calculations with ($\beta_2=0.54$) and without the effect of a deformation, respectively. (b) The corresponding $\rho(r)$.

1. Harmonic oscillator function

We investigated whether a harmonic oscillator (HO)-type $\rho(r)$ alone can describe the energy dependence of σ_R for ^{17}B. We calculated σ_R^{OL} using Eq. (2) with the finite-range parameter. The width parameter (a_{HO}) was chosen to reproduce the experimental data at high energy. We have tried two kinds of methods using the HO-type $\rho(r)$: one without the effect of a deformation, and the other with a deformation, where the deformation parameter (β_2) is calculated using

$$\beta_2=\frac{4\pi}{3ZeR_0^2}\sqrt{\frac{5}{16\pi}}Q_0, \tag{6}$$

with intrinsic quadrupole moment $Q_0=Q[(J+1)(2J+3)]/[J(2J-1)]$ and $R_0^2=0.0144A^{2/3}$ b [28]. The β_2 for ^{17}B was calculated to be 0.54 with the experimental Q moment $|Q(^{17}\mathrm{B})|=38.6\pm1.5$ mb [29]. The results are shown in Fig. 5(a).

It can be seen that neither calculation reproduces the data at intermediate energy and at high energy simultaneously. This situation differs from the case of ^{12}C. It is clear that the HO-type $\rho(r)$ alone can not reproduce the experimental σ_R of ^{17}B, even if it takes the deformation into account.

2. HO-type plus square of Yukawa function

We assumed $\rho(r)$ of ^{17}B to be a HO-type function for the core (^{15}B) plus a square of Yukawa function for the valence two-neutron, and calculated σ_R^{OL} with the finite-range parameter. The square of Yukawa function is known to be a good approximation to the shape of a single-particle density at an outer region of a core with centrifugal and Coulomb barriers. The assumed density is expressed as

$$\rho_p(r)=\text{HO type},\quad \rho_n(r)=\begin{cases}\text{HO type} & (r\leqslant r_c)\\ \rho_0\exp(-\lambda r)/r^2 & (r>r_c),\end{cases} \tag{7}$$

where r_c is the critical radius in which the HO-type function crosses with the square of Yukawa function; λ is the asymptotic slope of the tail and is used as the fitting parameter.

The r_c value was determined by a normalization process for the total number of neutrons. The a_{HO} of the core, chosen to be 1.679 fm so as to reproduce σ_I of ^{15}B [30], is common to both protons and neutrons. By fitting the measured σ_R with a free parameter (λ), the best fit was obtained with $\lambda=0.77$ and $\chi^2=8.03$. The best-fit curve for the energy dependence of σ_R and the resultant $\rho(r)$ are shown in Fig. 6. Since the minimum χ^2 value is not very small, the experimental uncertainty for $\rho(r)$ is chosen to reproduce data at both intermediate and high energy.

Here we have also considered the deformation of the core (^{15}B), itself. The β_2 for ^{15}B was calculated to be 0.57 using Eq. (6) with the experimental Q moment $|Q(^{15}\mathrm{B})|$

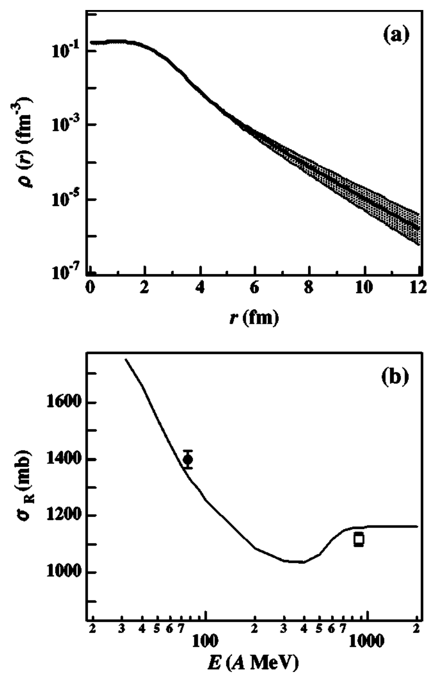

FIG. 6. (a) Density distribution of ^{17}B obtained via the OL approach. The hatched area shows the uncertainty. The upper limit of the error corresponds to the data at intermediate energy, and the lower limit of the error corresponds to that at high energy. (b) The resultant best-fit curve for the energy dependence of σ_R.

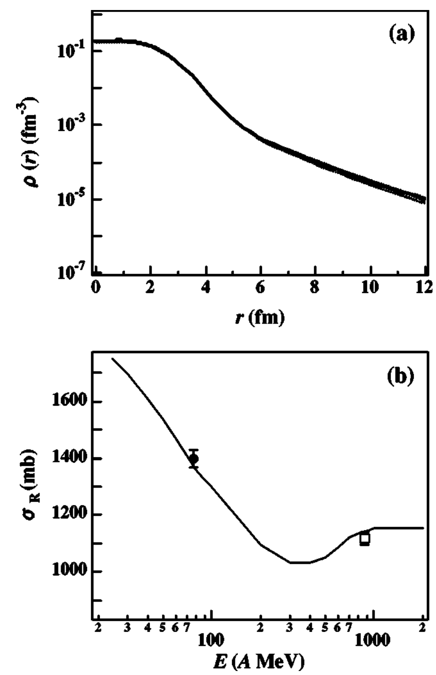

FIG. 7. Same as Fig. 6, but obtained via the FB approach.

$=38.01\pm 1.08$ mb [31]. We fitted the measured σ_R with a free parameter (λ) under core deformation. The best fit was obtained with $\lambda=0.68$ and $\chi^2=7.38$. The $\rho(r)$ value was almost the same as that in Fig. 6(a), since the minimum χ^2 value does not differ significantly from that obtained for the spherical core case.

3. Few-body Glauber calculation

It is pointed out that a few-body (FB) Glauber-type calculation may be more suitable to describe a weakly bound system, like a halo nucleus [25,32]. Thus, we applied the FB calculation to a three-body system (core+neutron+neutron) of ^{17}B. σ_R can be expressed as

$$\sigma_R^{\rm FB} = \int d\boldsymbol{b}[1 - |\langle\varphi_0|\exp\{i\chi_{FT}(\overline{\boldsymbol{b}}) + i\chi_{nT}(\overline{\boldsymbol{b}} + \boldsymbol{s}_1) + i\chi_{nT}(\overline{\boldsymbol{b}} + \boldsymbol{s}_2)\}|\varphi_0\rangle|^2], \tag{8}$$

where φ_0 denotes the wave function of a halo neutron; $\boldsymbol{s}_{1,2}$ is the halo neutron's vector from the core, perpendicular to the beam axis; $\overline{\boldsymbol{b}}$ $[=\boldsymbol{b}-(\boldsymbol{s}_1+\boldsymbol{s}_2)/17]$ denotes the impact parameter corresponding to a collision between the core and the target nucleus; χ_{FT} is the phase-shift function between the core and the target, and χ_{nT} is the phase-shift function between the halo neutron and the target. The finite-range parameter in the FB approach is the same as that used in the OL approach.

In this FB approach, $\rho(r)$ of ^{17}B was assumed as a HO-type function for the core (^{15}B) plus valence two neutrons. We have considered the $(2s_{1/2})^2_{J=0}$ or $(1d_{5/2})^2_{J=0}$ configurations for the valence two neutrons, i.e.,

$$\varphi(\boldsymbol{r}_1,\boldsymbol{r}_2) = [\phi_j(\boldsymbol{r}_1)\phi_j(\boldsymbol{r}_2)]_{J=0}, \tag{9}$$

where $j=2s_{1/2}$ or $1d_{5/2}$ and $\varphi(\boldsymbol{r}_1,\boldsymbol{r}_2)$ is the wave function of the valence two neutrons. The correlation of the two neutrons was not taken into account. Each wave function, $\phi_{2s_{1/2}}(\boldsymbol{r})$ and $\phi_{1d_{5/2}}(\boldsymbol{r})$, was determined by solving the eigenvalue problem of the Schrödinger equation in a Woods-Saxon potential for a given value of $S_{2n}/2$, with a diffuseness parameter of 0.7 fm and a radius parameter of $1.2A^{1/3}$ fm.

It was found that the pure $2s_{1/2}$ wave function overestimated the measured σ_R, and the pure $1d_{5/2}$ wave function underestimated it. We thus considered a mixed configuration as

$$\varphi(\boldsymbol{r}_1,\boldsymbol{r}_2) = \{\sqrt{f}[\phi_{2s_{1/2}}(\boldsymbol{r}_1)\phi_{2s_{1/2}}(\boldsymbol{r}_2)]_{J=0} + \sqrt{1-f}[\phi_{1d_{5/2}}(\boldsymbol{r}_1)\phi_{1d_{5/2}}(\boldsymbol{r}_2)]_{J=0}\}, \tag{10}$$

where $f(f\leqslant 1)$ denotes the s-wave spectroscopic factor [the fraction of the wave function with the valence two-neutron configuration of $(2s_{1/2})^2_{J=0}$ or $(1d_{5/2})^2_{J=0}$]. We fitted the measured σ_R with a free parameter (f). The minimum χ^2 was 2.53 with $f=0.5$. It should be noted that the minimum χ^2 value is better than that obtained via the OL approach. The resultant $\rho(r)$ and the best-fit curve for the energy dependence of σ_R are shown in Fig. 7. In this case, we determined the uncertainty of the density by taking the parameter at (χ^2+1).

The fraction parameter (f) was simultaneously found to be $50\pm 10\%$. In other words the s-wave component is crucial to the configuration for the valence two neutrons. This is consistent with a previous result $(69\pm 20\%)$ [17] within the experimental uncertainty.

C. Density distribution

We have applied the two methods described in the previous sections. In the present analysis, the FB approach reproduces the experimental data better than the OL approach from the point of the minimum χ^2 value. However, much more assumptions are involved in the FB approach, the wave function is assumed to be the product of the halo neutron wave function and the core wave function. Moreover, the slope of the tail is fixed by S_{2n}. In contrast, an advantage of the OL approach is the fact that the slope of the tail is independently determined from S_{2n}. Thus, it is difficult to decide which method should be better for ^{17}B density distribution. Therefore, we include, as the final $\rho(r)$ of ^{17}B, all distributions obtained from these two methods, and it is shown in Fig. 8. It is clearly demonstrated that a long neutron tail with a significant amplitude exists in the density distribution of ^{17}B.

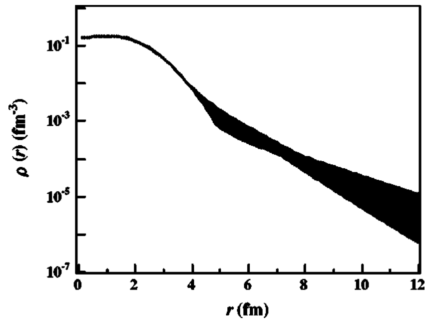

FIG. 8. Final density distribution of ^{17}B with a significant amplitude of a long neutron tail.

IV. SUMMARY

We have measured the reaction cross section for ^{17}B on a carbon reaction target at an energy of 77*A* MeV by a transmission method. Based on the assumption of a core (^{15}B) plus valence two-neutron picture, the density distribution of ^{17}B was deduced through the energy dependence of the reaction cross section using a Glauber-type calculation.

We employed the finite-range Glauber-type calculation under the optical-limit approximation as well as the few-body approach. The new finite-range parameter in the profile function is parameterized by using the energy dependence of σ_R for the ^{12}C+^{12}C system.

It was proved that the neutron tail in the density distribution is essential for ^{17}B to reproduce the measured reaction cross sections. The existence of the long neutron tail in ^{17}B was demonstrated for the first time. The fraction of the wave function with the valence two-neutron configuration of $(2s_{1/2})^2_{J=0}$ or $(1d_{5/2})^2_{J=0}$ was found to be $50\pm10\%$ under the finite-range few-body Glauber-type calculation. The *s*-wave component is crucial to the configuration for the valence two neutrons in ^{17}B, and can be understood to be one of the phenomena required for neutron halo formation.

ACKNOWLEDGEMENT

The authors gratefully acknowledge all of the staff at the RIKEN ring cyclotron for their stable operation of the accelerator during the experiment. We thank Dr. J. Miller at LBL for his careful reading of the manuscript.

[1] I. Tanihata, H. Hamagaki, O. Hashimoto, Y. Shida, N. Yoshikawa, K. Sugimoto, O. Yamakawa, T. Kobayashi, and N. Takahashi, Phys. Rev. Lett. **55**, 2676 (1985).
[2] P. G. Hansen and B. Jonson, Europhys. Lett. **4**, 409 (1987).
[3] I. Tanihata, T. Kobayashi, O. Yamakawa, S. Shimoura, K. Ekuni, K. Sugimoto, N. Takahashi, T. Shimoda, and H. Sato, Phys. Lett. B **206**, 592 (1988).
[4] T. Kobayashi, O. Yamakawa, K. Omata, K. Sugimoto, T. Shimoda, N. Takahashi, and I. Tanihata, Phys. Rev. Lett. **60**, 2599 (1988).
[5] M. Fukuda *et al.*, Phys. Lett. B **268**, 339 (1991).
[6] I. Tanihata, Nucl. Phys. **A522**, 275c (1991).
[7] I. Tanihata *et al.*, Phys. Lett. B **287**, 307 (1992).
[8] S. Fortier *et al.*, Phys. Lett. B **461**, 22 (1999).
[9] H. Simon *et al.*, Phys. Rev. Lett. **83**, 496 (1999).
[10] W. Geithner *et al.*, Phys. Rev. Lett. **83**, 3792 (1999).
[11] T. Aumann *et al.*, Phys. Rev. Lett. **84**, 35 (2000).
[12] J. P. Dufour *et al.*, Phys. Lett. B **206**, 195 (1988).
[13] Z. Ren and G. Xu, Phys. Lett. B **252**, 311 (1990).
[14] K. Riisager, D. V. Fedorov and A. S. Jensen, Europhys. Lett. **49**, 547 (2000).
[15] G. Audi, O. Bersillon, J. Blachot and A. H. Wapstra, Nucl. Phys. **A624**, 1 (1997).
[16] T. Suzuki *et al.*, Nucl. Phys. **A658**, 313 (1999).
[17] T. Suzuki *et al.*, Phys. Rev. Lett. **89**, 012501 (2002).
[18] T. Kubo, M. Ishihara, N. Inabe, H. Kumagai, I. Tanihata, K. Yoshida, T. Nakamura, H. Okuno, S. Shimoura, and K. Asahi, Nucl. Instrum. Methods Phys. Res. B **70**, 309 (1992).
[19] H. Kumagai, A. Ozawa, N. Fukuda, K. Sümmerer, and I. Tanihata, Nucl. Instrum. Methods Phys. Res. A **470**, 562 (2001).
[20] K. Kimura *et al.*, Nucl. Instrum. and Meth. A (to be published).
[21] C. Wu *et al.*, Nucl. Phys. **A739**, 3 (2004).
[22] S. Kox *et al.*, Phys. Rev. C **35**, 1678 (1987).
[23] A. Ozawa *et al.*, Nucl. Phys. **A709**, 60 (2002).
[24] T. Zheng *et al.*, Nucl. Phys. **A709**, 103 (2002).
[25] Y. Ogawa, T. Kido, K. Yabana and Y. Suzuki, Prog. Theor. Phys. Suppl. **142**, 157 (2001).
[26] M. Fukuda (private communication).
[27] A. Ozawa *et al.*, Nucl. Phys. **A691**, 599 (2001).
[28] S. Raman, C. H. Malarkey, W. T. Milner, C. W. Nestor, Jr., and P. H. Stelson, At. Data Nucl. Data Tables **36**, 1 (1987).
[29] H. Ogawa *et al.*, Phys. Rev. C **67**, 064308 (2003).
[30] A. Ozawa, I. Tanihata, T. Kobayashi, Y. Sugahara, O. Yamakawa, K. Omata, K. Sugimoto, D. Olson, W. Christie, and H. Wieman, Nucl. Phys. **A608**, 63 (1996).
[31] H. Izumi *et al.*, Phys. Lett. B **366**, 51 (1996).
[32] J. S. Al-Khalili, J. A. Tostevin and I. J. Thompson, Phys. Rev. C **54**, 1843 (1996).